

DESIGN STUDY FOR A 205 MEV ENERGY RECOVERY LINAC TEST FACILITY AT THE KEK

Eun-San Kim, Pohang Accelerator Lab., POSTECH, Pohang, 790-784 Korea
 Kaoru Yokoya, KEK, 1-1 Oho, Tsukuba, Ibaraki, 305-0801 Japan

Abstract

We present design of lattices and beam dynamics analysis for a 205 MeV energy recovery linac test facility at the KEK. The test facility consists of a photocathode rf gun, a 5 MeV injector, a merger, a 205 MeV superconducting rf linac, triple bend achromats and beam dump line. Beam parameters and optimal optics to realize the energy recovery linac are investigated. Two kinds of lattices for the arcs are designed: an isochronous lattice and a lattice for bunch compression. Simulation results on emittance growth due to HOMs in the superconducting rf linac and coherent synchrotron radiation in the designed lattices are presented.

INTRODUCTION

Energy recovery linac (ERL) has been widely studied as high efficiency accelerators for next generation light sources[1]. ERL design study at the KEK also showed the feasibility of a new synchrotron light source based on a 5 GeV superconducting linac. It was shown in the design study that considerable investigations in the accelerator physics issues and technological development were required in order to achieve small emittance, flux, brilliance, and short pulse in the ERL facility[2]. Accordingly, it was proposed to construct a 205 MeV test facility at the KEK in which required beam parameters could be demonstrated and most of the accelerator technology issues would be realized.

In this paper, we present the results on design studies that were performed for the ERL test facility at the KEK. We can divide the test facility into four major parts: injector, main linac, arcs and beam dump line. The injector includes a photocathode RF gun, linac that raise the energy of the beam to 5 MeV and merger. We do not perform energy recovery for this stage. The main linac consists of 10 superconducting rf cavities to accelerate the beam energy to 205 MeV. Isochronous arcs as well as arcs that act as a compressor and decompressor are designed. We present major points of the our optics design: First is compensation of emittance growth due to the coherent synchrotron radiation (CSR) in the merger, second is the triple bend achromats that can easily control the magnitude of R_{56} , and third is to produce zero dispersion function for insertion device in straight section and designed optics is symmetric at the center of the straight section. Fourth, the optics of beam dump line has the mirror image of the injection merger. We also present the results of the simulations performed on the beam breakup in the designed ERL test facility.

CHARACTERISTICS OF THE ERL TEST FACILITY

A layout for the designed ERL test facility is shown in Fig.1. The injector section increases the energy of the beam to 5 MeV where the space charge effect is greatly reduced. A 5 MeV electron beam with normalized transverse emittance of 0.1 mm-mrad is injected into the 1.29 GHz superconducting rf main linac. Each rf bucket in the linac is completely filled out and the average beam current is 100 mA. Low charge of 77 pC per bunch is chosen to make weaken the effects of the CSR, space charge, and wakefields on the emittance growth that may be caused due to high bunch charges. The bunch with rms bunch length of 1 ps can be compressed down to around 200 fs in the achromat with variable R_{56} . Then the beam goes through the straight section of 36 m long where it can be used to produce UV. The beam is then returned to the main linac with a 180° rf phase offset for energy recovery. In the main linac the beam releases their energy for the acceleration of injected bunches. Finally, the beam of 5 MeV energy exits the main linac and is toward to a beam dump line. Table 1 shows the main parameters of the designed ERL test facility.

MERGER

Two things are considered for the design of the merger: minimization of growth of transverse emittance due to the CSR effect and matching of betatron functions to the entrance of the main linac. Designed optics for the merger consists of four quadrupoles and four dipoles. A layout for the merger is shown in Fig. 2. The rf cavities in the main linac have a high accelerating gradient of 20MV/m and so a 5 MeV beam sees strong rf focusing in the entrance of the main linac. Thus, we designed to make the betatron function in the entrance of the main linac small in order to produce a small beam envelope at the entrance of the main linac. It is designed that bending angle in the dipoles becomes as small as possible to minimize emittance growth due to the CSR effect. Four dipole magnets with 10 degree introduce the beam to the main linac. The bending section is achromatic and four dipoles with each length of 0.3 m are identical rectangular magnets. Four quadrupoles with each length of 0.15 m are utilized for the matching of the betatron function of the injector lattice into the main linac.

LINAC

A single triplet focusing is located at the center of the main linac. Both injected and returned beams have almost the same energy and feel the same focusing in the center of

the main linac. The main linac consists of two cryomodules in which each cryomodule has five rf cavities. The effects of long-range wake and short-range wake due to HOMs in the cavities on the beam instabilities are investigated by a simulation method. Transverse HOMs in the rf cavities that are considered in our simulations are listed in Table 2. Dependence of beam breakup on locations of rf HOMs frequencies is also investigated. Long-range wake is considered by a resonant model and its wake function is given by

$$W_T(z) = \frac{w_o R/Q}{\sqrt{1 - 1/4Q^2}} e^{-w_o z/2cQ} \sin(w_o z/c\sqrt{1 - 1/4Q^2}). \quad (1)$$

Wake function of short-range wake is given by

$$W_T(z) = zW_o[(1 + c_o)\exp(-\sqrt{z/z_o}) - c_o] \quad (2)$$

Here, $W_o=38.1 \times 10^{12}$, $c_o=0.165$ and $z_o=3.65 \times 10^{-3}$.

TRIPLE BEND ACHROMATS

The optics for the arcs has the structure of the triple bend achromat (TBA) cell. It is chosen due to the fact that R_{56} in the arc is easily adjustable for the compression and decompression of the beam. This can be performed by varying the dispersion function in the center of the arc. Each dipole has a length of 0.5 m and its bending angle is 45 degree. We optimized the optics of arcs so that emittance growth due to the CSR in the arcs is to be acceptably small. We designed two kinds of TBAs with R_{56} of 10^{-5} and -0.15, as shown in Fig. 3 and Fig. 4, respectively, which also include the optics from the merger to beam dump line.

BEAM BREAKUP DUE TO COHERENT SYNCHROTRON RADIATION AND RF HOMS

The effect of incoherent synchrotron radiation in the test facility is estimated to be very small. However, the effects of the CSR on the machine performances are shown to be large. The CSR energy loss, U_d , per electron in a dipole magnet, and bending radius, ρ , for a bunch with a Gaussian distribution is estimated using the following formula:

$$U_d(\text{eV}) = 998 \frac{q(\text{pC})}{\sigma_z(\text{mm})^{4/3}} \rho(\text{m})^{1/3} \frac{\theta(\text{deg})}{360^\circ}, \quad (3)$$

where q is the charge per bunch, σ_z is the rms bunch length and θ is the dipole bending angle. The total CSR power loss is given by $P_{CSR}(W) = U_d(\text{eV})I(A)$, where I is the beam current. Table 3 shows estimate of power loss due to the CSR in the merger and beam dump line, and two arcs.

Start-to-end beam simulations (from merger to beam dump line) were also performed to investigate the beam breakup due to the CSR and RF HOMs. Fig. 5 shows variations of the horizontal (top) and vertical (bottom) emittances for 320 bunches in the optics of $R_{56}=10^{-5}$. Fig.

6 shows variations of average longitudinal beam position (top) and rms bunch length (bottom) for the optics of $R_{56}=10^{-5}$. Fig. 7 shows variations of the horizontal (top) and vertical (bottom) emittances for 320 bunches in the optics of $R_{56}=-0.15$. Initial horizontal beam emittance is 0.1 mm-mrad and it is shown that the beam emittance increases to around 0.4 mm-mrad due to the effects of the CSR and rf HOMs in the designed lattices.

Table 1: Main parameters of the designed ERL test facility

| Parameter | Unit | Value |
|---------------------------|---------|--------------------|
| Energy | MeV | 205 |
| Total length | m | 112.78 |
| Initial rms bunch length | ps | 1 |
| Energy pread | | 3×10^{-4} |
| Charge per bunch | pC | 77 |
| Average beam current | mA | 100 |
| Injection energy | MeV | 5 |
| Normalized emittance(H/V) | mm-mrad | 0.1/0.1 |
| Fundamental rf frequency | GHz | 1.2961 |
| R_{56} in one arc | | 10^{-5} , -0.15 |
| Harmonic number | | 320 |

Table 2: Considered transverse rf HOMs

| f [GHz] | R/Q [Ω/m^2] | Q |
|---------|----------------------|-------|
| 2.57535 | 238000 | 50000 |
| 1.8722 | 86900 | 70000 |
| 1.8643 | 65400 | 50000 |

Table 3: Estimate of CSR power loss in the designed ERL

| Parameter | θ | ρ | σ_z | P_{CSR} |
|-------------|-------------|---------|------------|-----------|
| Merger+Dump | 80° | 1.71 m | 1 ps | 10.2 kW |
| 2 Arcs | 360° | 0.636 m | 1 ps | 32.8 kW |

CONCLUSION

We have described studies on optic design for a 205 MeV energy recovery linac test facility. We presented a study of the beam breakup instability due to the CSR and rf HOMs in the proposed ERL test facility. It is also known by the simulations that locations of rf HOM frequencies have an effect on the magnitudes of beam breakup. It is shown through our design studies that goals of beam parameters for the proposed test facility are achievable and more optimization works are also needed.

REFERENCES

- [1] Ivan Bazarov et al, JLAB-ACT-01-04 (2001).
- [2] Study Report on Future Light Source at the Photon Factory (in Japanese) (2003).

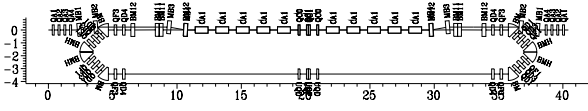


Figure 1: Layout of the 205 MeV ERL test facility.

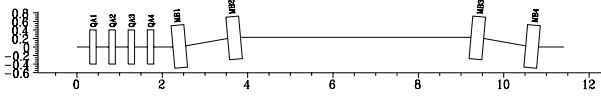


Figure 2: Layout of merger section between the 5 MeV linac and the main linac.

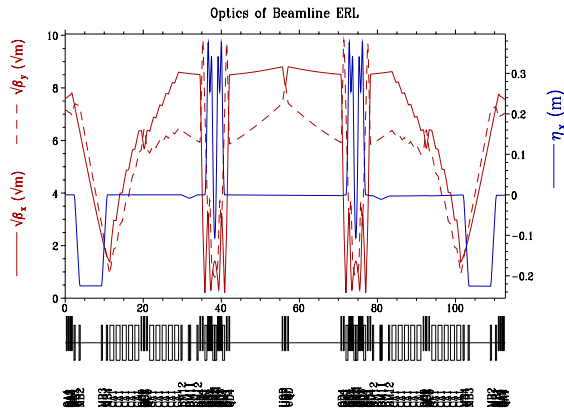


Figure 3: Optics from merger to beam dump line. R_{56} is 10^{-5} .

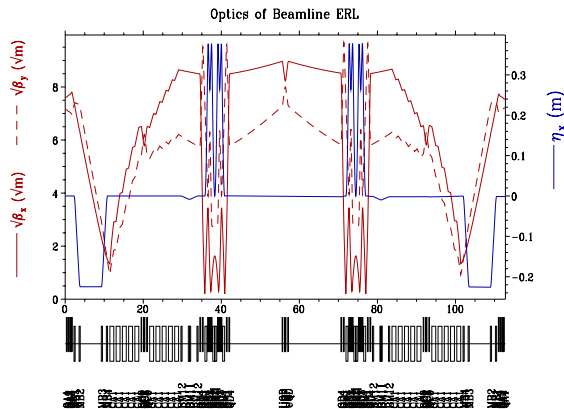


Figure 4: Optics from merger to beam dump line. R_{56} is -0.15 .

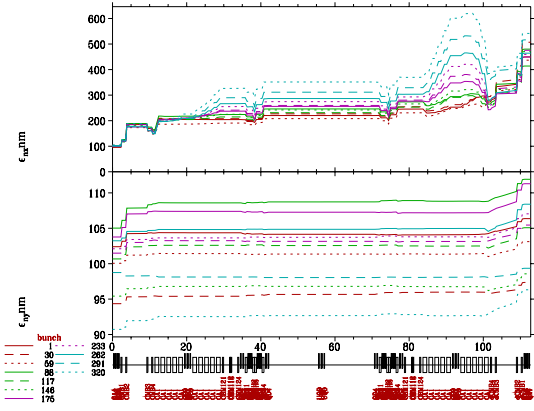


Figure 5: Variations of horizontal (top) and vertical (bottom) emittances for 320 bunches in the optics of $R_{56}=10^{-5}$.

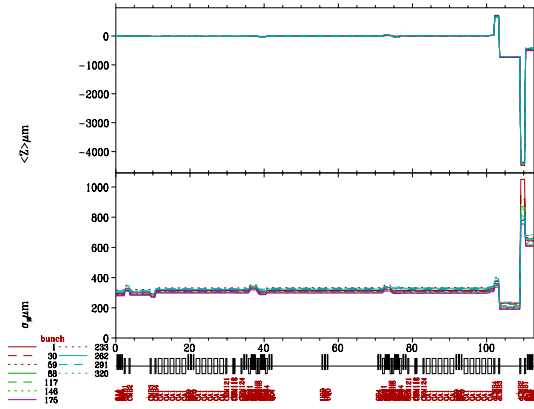


Figure 6: Variations of average longitudinal beam position (top) and rms bunch length (bottom) for 320 bunches in the optics of $R_{56}=10^{-5}$.

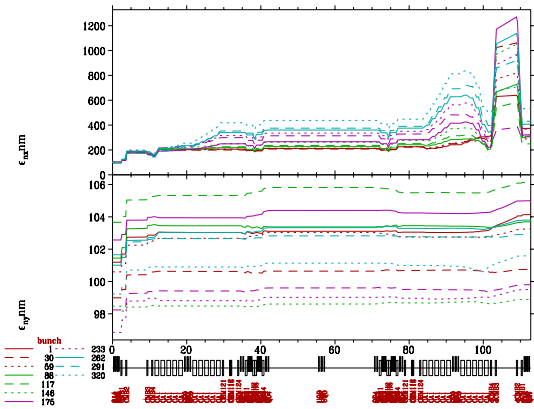


Figure 7: Variations of horizontal (top) and vertical (bottom) emittances for 320 bunches in the optics of $R_{56}=-0.15$.